This is a repository copy of *Computational studies into urea formation in the interstellar medium*.

White Rose Research Online URL for this paper:
http://eprints.whiterose.ac.uk/166942/

Version: Published Version

Article:

Slate, E.C.S., Barker, R., Euesden, R.T. et al. (2 more authors) (2020) Computational studies into urea formation in the interstellar medium. Monthly Notices of the Royal Astronomical Society, 497 (4). pp. 5413-5420. ISSN 0035-8711

https://doi.org/10.1093/mnras/staa2436

This article has been accepted for publication in Monthly Notices of the Royal Astronomical Society ©: 2020 The Author(s). Published by Oxford University Press on behalf of the Royal Astronomical Society. All rights reserved.

Reuse

Items deposited in White Rose Research Online are protected by copyright, with all rights reserved unless indicated otherwise. They may be downloaded and/or printed for private study, or other acts as permitted by national copyright laws. The publisher or other rights holders may allow further reproduction and re-use of the full text version. This is indicated by the licence information on the White Rose Research Online record for the item.

Takedown

If you consider content in White Rose Research Online to be in breach of UK law, please notify us by emailing eprints@whiterose.ac.uk including the URL of the record and the reason for the withdrawal request.

eprints@whiterose.ac.uk
https://eprints.whiterose.ac.uk/

Monthly Notices
of the
ROYAL ASTRONOMICAL SOCIETY

MNRAS **497,** 5413–5420 (2020) doi:10.1093/mnras/staa2436
Advance Access publication 2020 August 14

Computational studies into urea formation in the interstellar medium

Eren C. S. Slate,[★] Rory Barker, Ryan T. Euesden, Max R. Revels and Anthony J. H. M. Meijer
Department of Chemistry, University of Sheffield, Brook Hill, Sheffield S3 7HF, UK

Accepted 2020 August 5. Received 2020 August 5; in original form 2020 June 5

ABSTRACT

Formation routes, involving closed shell, radical, and charged species for urea, have been studied using computational methods to probe their feasibility in the interstellar medium. All reactions involving closed shell species were found to have prohibitive barriers. The radical–radical reaction possesses a barrier of only 4 kJ mol^{-1}, which could be surmountable. A charged species based route was also investigated. A barrier of only 8 kJ mol^{-1} was found in that case, when a partial water ice shell was included.

Key words: astrochemistry – ISM: clouds – ISM: general – ISM: molecules.

1 INTRODUCTION

To date around 200 molecules have been detected in the interstellar medium or in circumstellar shells (Köln Database: https://cdms.astro.uni-koeln.de/classic/molecules, last visited 2020 August 24) (Ehrenfreund & Charnley 2000; Tielens 2013). Such detections prompt the question of how these molecules form in interstellar environments under significantly different conditions to their formation on Earth. In particular, both temperature and pressure will be lower in the interstellar medium (ISM; Shaw 2007). As a consequence, much research has been directed towards studying the formation of molecules in the gas phase in the ISM and also towards the chemistry taking place on the surfaces of dust grains found in space (Garrod & Herbst 2006; Garrod, Weaver & Herbst 2008; Wakelam et al. 2015; Altwegg et al. 2016; Gorai et al. 2017; Holdship et al. 2019). One particular subset of ISM molecules that are of interest to us here are those with biological relevance as these may shed light on the beginnings of life (Orgel 1986; Jørgensen et al. 2012; Fray et al. 2016).

A key component of life on Earth are proteins, which can be viewed as polymers of peptides connected by so-called peptide bonds. Urea, $CO(NH_2)_2$, is one of the simplest molecules with such a peptide bond. Terrestrially, it is the waste product of a variety of biological functions and is often used as a fertilizer. It was the first biological molecule to be produced entirely abiotically (Wöhler 1828) and it is viewed as a potentially important molecule in the abiotic origin of life. Moreover, it was one of the identified products of the now famous Urey–Miller experiment in the 1950s (Miller & Urey 1959). A subsequent experiment, for the prebiotic formation of pyrimidines, by Robertson and Miller, further showed the relevance of urea to the origins of life field (Robertson & Miller 1995). Robertson and Miller showed that urea can act as a carbon source in the formation of cytosine and uracil via the scheme given in Fig. 1 (Jeilani, Fearce & Nguyen 2015). The biological relevance of these two nucleotides is clear and fits in with the proposed RNA world hypothesis for the Origins of Life on Earth (Alberts et al. 2002).

Thus, in the current models for the formation of biologically relevant molecules in the ISM, urea plays a key role. Therefore, it is important to know how urea is formed. Initially, it was thought that it may have formed on early Earth. In particular, it was thought that a Wöhler-type synthesis mechanism (Kinne-Saffran & Kinne 1999) would account for the presence of urea. A Wöhler-type synthesis starts from $NH_4(OCN)$, which then dissociates into ammonia and HOCN upon heating. These species then react to form urea; see equation (1) (Kinne-Saffran & Kinne 1999):

$$NH_4(OCN) \longrightarrow NH_3 + HOCN \rightleftharpoons (NH_2)_2CO. \quad (1)$$

However, there are some concerns over this mechanism. For example, concentrations of ammonium cyanate on early Earth are thought to be low. This is compounded by the fact that cyanates are not stable in water over geological time-scales. Thus, the amount of cyanate present would be limited. As a consequence, this formation route for urea would be difficult (Miller & Orgel 1974). Therefore, alternative routes to terrestrial formation need to be considered. One alternative is that urea was formed in space and brought to Earth through cometary impacts. The identification of urea on the Murchison meteorite, along with amino acids and nuclear bases, lends credence to this theory (Hayatsu et al. 1975). However, even though a tentative detection was made by Raunier et al. (2004), urea has proven to be quite elusive (Raunier et al. 2004; Remijan et al. 2014), although experiments using model ices as well as chemical networks have suggested that a variety of amines and amides should be present in the ISM, meaning that urea should be formed readily. This was shown by a recent detection of urea towards Sag B2(N1) by Belloche et al. (2019).

Urea has only been detected in a single source at a low density. However, its close analogues formamide, acetamide, and methylamine have all been found to be reasonably abundant in the ISM. Formamide, in particular, is a possible precursor to urea (Rubin et al. 1971; Fourikis, Takagi & Morimoto 1974; Hollis et al. 2006). In laboratory experiments, urea has been synthesized in model ices irradiated to mimic the effect of galactic cosmic rays (GCRs) and high-energy ultraviolet (UV) present in the ISM. Raunier et al. studied the formation of urea through the irradiation of solid

---

[★] E-mail: a.meijer@sheffield.ac.uk

© 2020 The Author(s)
Published by Oxford University Press on behalf of the Royal Astronomical Society

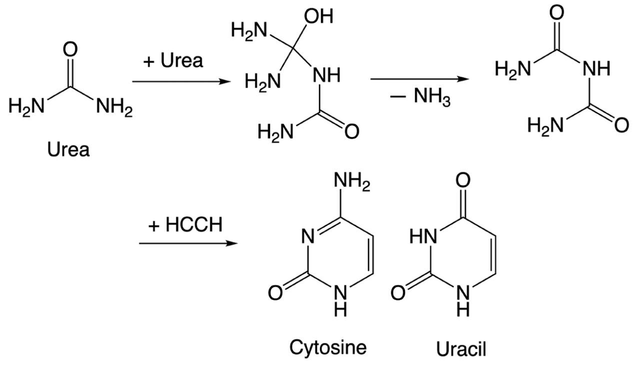

Figure 1. The reaction of urea with itself to ultimately yield the nuclear bases cytosine and uracil.

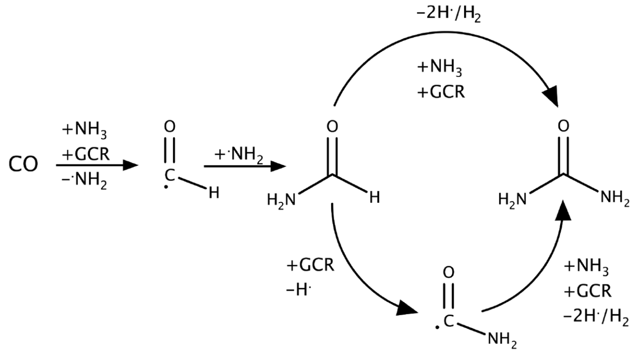

Figure 2. The possible mechanisms for the formation of urea from formamide and ammonia proposed by Förstel et al. (2016) (Adapted from Förstel et al. (2016) with permission from the Royal Society of Chemistry).

isocyanic acid (HNCO). They showed that such irradiation leads to the formation of both formamide and urea (Raunier et al. 2004). Additionally, they found evidence of the formation of NH_4OCN, suggesting that the break-up of isocyanic acid leads to the formation of ammonia, which combines readily with remaining isocyanic acid, as had been shown before (Raunier et al. 2003). However, the exact mechanism for the formation of urea has yet to be determined (Förstel et al. 2016). As noted in model ice experiments both formamide and urea have been detected. This suggests that formamide could be an intermediate in the formation of urea. Based on this hypothesis, two potential mechanisms have been suggested by Förstel et al. (2016). These proposals are outlined in Fig. 2.

The successful detection of formamide in the ISM and the wealth of existing work on the formation thereof means that the way in which it is produced in the ISM is not probed in this work (Redondo, Barrientos & Largo 2013; Kaňuchová et al. 2016; Song & Kästner 2016; Spezia et al. 2016; Dulieu et al. 2019). Instead, this work aims to use computational means to test the feasibility of these proposed mechanisms for converting formamide into urea, as well as alternatives based on radical and charged species chemistry, for the formation of urea from formamide and ammonia under astrochemical conditions. For a full list of the reactions considered herein, see Table 1. In particular, these reactions are being investigated as if they were occurring on an icy dust grain. As water ice is the dominant ice component within the ISM in this work, H_2O molecules are used to mimic such a mantle.

Table 1. The various reactions being investigated in this paper for their ability to produce urea on the surface of icy duct grains in the ISM.

$H_2NCOH + NH_3 \longrightarrow (H_2N)_2CO + H_2$
$H_2NCOH \longrightarrow H_2NCO\cdot + H\cdot$
$H_2NCO\cdot + NH_3 \longrightarrow (H_2N)_2CO + H\cdot$
$H_2NCO\cdot + .NH_2 \longrightarrow (H_2N)_2CO$
$H_2NCOH + .NH_2 \longrightarrow (H_2N)_2CO + H\cdot$
$HOCNH^+ + NH_3 \longrightarrow (H_2N)_2CO + H^+$
$OCNH_2{}^+ + NH_3 \longrightarrow (H_2N)_2CO + H^+$

Table 2. The number of CSFs in each RASSCF calculation.

Reaction	Number of CSFs
$H_2NCHO + H_2N^\bullet$	182 182
$H_2NCO^\bullet + H_3N$	182 182
$H_2NCO^\bullet + H_2N^\bullet$	89 232

2 METHODOLOGY

Calculations were carried out using the MOLPRO suite of *ab initio* programmes (Werner et al. 2012) using the MCSCF/RASSCF programmes and the 6-311G(d,p) basis set (Krishnan et al. 1980; McLean & Chandler 1980). Subsidiary calculations were performed using the GAUSSIAN09 suite of electronic structure programmes (Frisch et al. 2009) using DFT with the CAM-B3LYP functional (Lee, Yang & Parr 1988; Becke 1993; Yanai, Tew & Handy 2004) using a 6-311G(d,p) basis.

For the reactions containing radicals, the geometries of all identified product species were optimized first. Subsequently, a series of calculations were carried out in MOLPRO using the MCSCF/RASSCF programmes. In these calculations, the reactant species were placed at a maximum interreactant distance of 5 Å and the distance decreased in steps of either 0.1 or 0.2 Å. The geometries, except for any variables required to maintain the angle of approach for the incoming radical and the interradical distance, were re-optimized at the Hartree–Fock level at each step. A restricted active space was used for these calculations, where orbitals with occupation numbers higher than 1.98 were closed so that they were doubly occupied. Those orbitals with occupancies lower than 0.2 were restricted to have no more than two electrons in total in them, but were left active (Krishnan et al. 1980; McLean & Chandler 1980; Knowles & Werner 1985; Werner & Knowles 1985; Frisch, Head-Gordon & Pople 1990a,b; Werner et al. 2012). No RAS3 space was used in any of our calculations. An indication of the size of the active space and the number of CSFs included is given in Table 2.

For the reactions involving charged species, relaxed scans using redundant coordinates in GAUSSIAN09 were used to scan over the interreactant distance in steps of 0.1 Å with the geometries being re-optimized at each interval at the CAM-B3LYP/6-311G(d,p) level (Lee et al. 1988; Becke 1993; Yanai et al. 2004)

3 RESULTS AND DISCUSSION

3.1 Förstel mechanism

3.1.1 Closed shell pathway

The mechanisms proposed by Förstel and coworkers were introduced earlier (Förstel et al. 2016). It is these mechanisms that form the basis of the radical-based mechanisms investigated in this work. Fig. 3 outlines the various formation pathways to urea including one

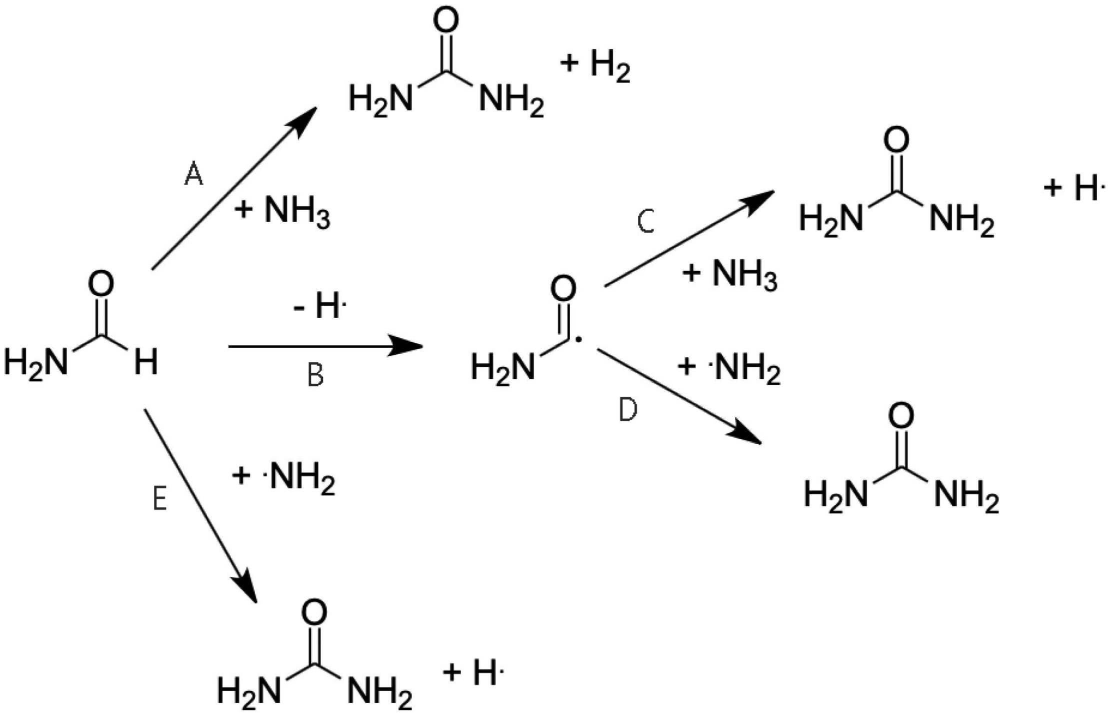

Figure 3. Pathways to urea formation from formamide probed during this work, based on those proposed by Förstel et al. (2016).

concerted reaction between formamide and ammonia (pathway A), which is identical to the top pathway in Fig. 2. To try and confirm the whether this reaction route involving only closed shell molecules was possible, the structures were optimized using DFT. Subsequently, high-accuracy CCSD(T) energy calculations were carried out on the optimized products and reactants of this proposed mechanism step. The results of these calculations in the gas phase show that the formation of urea and dihydrogen from formamide and ammonia is endothermic by 26 kJ mol^{-1}. However, the inclusion of the zero-point energy correction reduces the endothermicity to 8 kJ mol^{-1}, an amount that could be surmountable in the ISM. Unfortunately, the transition state could not be located, which means that the viability of this pathway is unclear. However, as it involves the breaking and forming of strong covalent bonds, it is anticipated to be substantial. As a consequence this pathway was not pursued any further.

3.1.2 *Single radical pathways*

The alternative reaction mechanism for the formation of urea given by Förstel et al. (2016) uses a formamide radical and ammonia as the reactants; see pathway B in Fig. 3. Radical reactions are prevalent in the ISM and contribute to the formation of many COMs making this a priori a formation pathway, which should be investigated (Ashfold et al. 2019; Butscher et al. 2019; Sharma 2019; Zhao et al. 2019). Indeed, the formamide radical has been detected in matrix-isolation studies (Pettersson et al. 1999). First, the dissociation of formamide to yield the radical species was investigated. The process was found to be barrierless and require an energy input of 678 kJ mol^{-1} (7.0 eV) when a partial water shell was included in the system to mimic an ice mantle. Alternatively, the hydrogen could be abstracted by a neighbouring OH, which would be a barrier possessing process. However, it may be possible for the hydrogen to successfully tunnel across any such barrier. Processes like this have already been shown to produce radicals in ice mantles (Garrod & Weaver 2013).

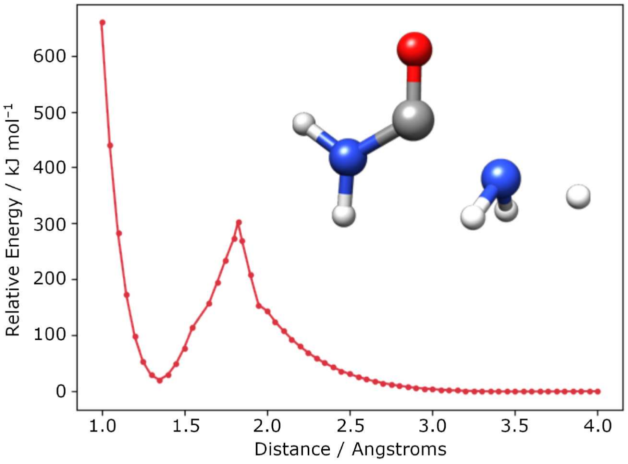

Figure 4. The potential energy curve for the addition of ammonia to formamide radical in the gas phase to give urea as calculated by RASSCF where the energy at a radical distance of 4 Å is taken as the zero. Inset: the optimized structure at an interreactant distance of 1.825 Å corresponding to the peak of the barrier in the potential energy curve calculated by RASSCF for formamide radical reacting with ammonia.

RASSCF calculations were subsequently carried out to follow the reaction between the formamide radical and ammonia; see step C in Fig. 3. In the calculations, the CN bond was used as the reaction coordinate and the structures were re-optimized at each step. The potential energy curve for this reaction is given by Fig. 4. Here, urea is observed to form, along with a hydrogen radical. However, the products are higher in energy than the reactants by 20 kJ mol^{-1}. Additionally, there appears to be a substantial barrier to the formation of the products of 282 kJ mol^{-1}. Inspection of the transition state structure (inset in Fig. 4) shows that the barrier corresponds to the

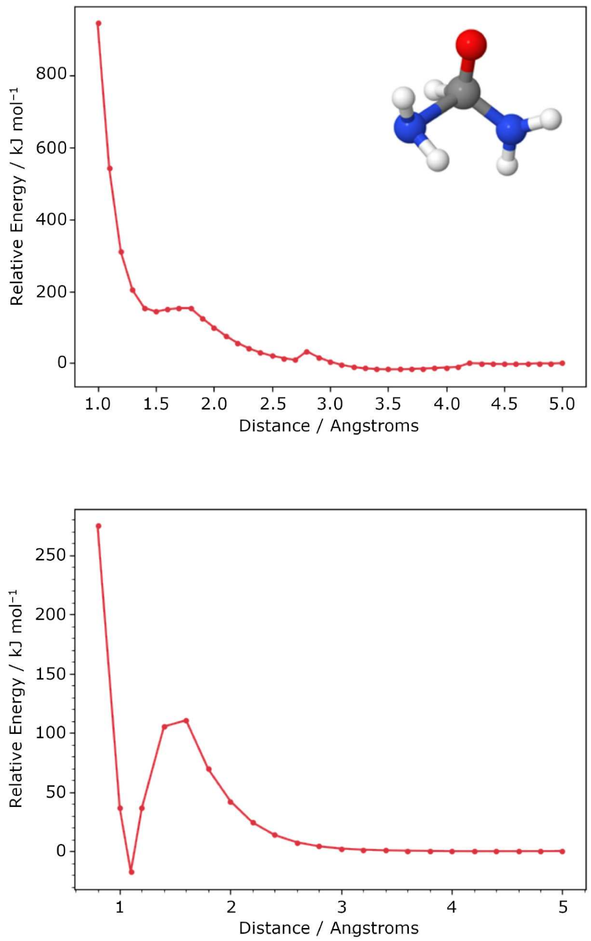

Figure 5. Top panel: the potential energy curve for the addition of an amino radical to formamide in the gas phase to give urea, as calculated by RASSCF where the energy at a radical distance of 5 Å is taken as the zero. Inset: the optimized structure of the intermediate at 1.5 Å in the potential energy curve for the formation of urea from an amino radical and formamide. Bottom panel: the potential energy curve for the dissociation of the CH bond in the high-energy intermediate given from the reaction between formamide and an amino radical. Here, the energy of the system at a separation of 5 Å taken as the zero.

mid-point of NH bond cleavage and CN bond formation. After this point, the ammonia nitrogen forms a CN bond with formamide to make urea and the hydrogen radical formed departs. The small discontinuity in the gradient of the potential energy curve at 1.55 Å corresponds to a small geometric change in the system. At this point, the incoming nitrogen atom switches from a trigonal arrangement, as found in ammonia, to the planar NH_2 group found in urea.

Clearly, this particular route to urea is unlikely under astrochemical conditions, given its endothermicity and the sizeable barrier. Thus, alternatives were considered. One such possibility would be to use formamide and an amino radical (step E in Fig. 3) as opposed to the formamide being the radical species. A scan of the CN distance for these reactant species was performed. The potential energy curve, top panel in Fig. 5, shows no large barrier. However, the reaction is endothermic. The dip in the energy curve at approximately 3.5 Å is caused by the formation of favourable interactions between the amino radical and the formamide carbonyl and amino group, forming a six-membered hydrogen-bonded ring. The disruption of these interactions as the CN intermolecular distance decreases causes the small barrier at 2.8 Å. The increase in energy from 2.7 Å onwards is caused by the incoming amino radical distorting the shape of formamide and thus breaking the π-delocalization. The energy of this transition state is 150 kJ mol^{-1} above the initial, well-separated species. The second dip in energy at 1.5 Å represents a high-energy intermediate and does not correspond to the formation of urea. The optimized structure at this point is shown in the inset in the upper panel of Fig. 5.

As can be seen, the formamide CH bond does not cleave to yield the target product of urea. Thus, a scan of the CH bond was performed starting from the structure shown in the inset in the upper panel of Fig. 5. The resulting potential energy curve is given in the lower panel of Fig. 5. This process displays another barrier of 108 kJ mol^{-1}. This transition state corresponds to the point, where the incoming nitrogen atom makes a geometric change from tetrahedral to the planar structure seen in urea. The potential energy curve then plateaus after the formation of urea and a hydrogen radical. The products in case are 18 kJ mol^{-1} less stable than the tetrahedral intermediate species. The endothermicity of the reaction as well as the height of the two barriers make this an unlikely formation route under ISM conditions. It is also worth noting that, with this reaction, there is the chance for a competing reaction in which the amino radical abstracts a hydrogen from the formamide to yield ammonia and a formamide radical. This competing option has not been investigated here as the feasibility of the target reaction is already low. In light of all of this, we investigated a number of other formation pathways as well.

3.2 Radical–radical pathway

The substantial barriers to the formation of urea from either formamide or amino radicals make these unlikely formation pathways in the ISM. However, an obvious further option is to use both a formamide radical and an amino radical to form urea (pathway D in Fig. 3), since radical–radical reactions contribute to the presence of many COMs in the ISM (Öberg 2016; Butscher et al. 2017). Indeed, this reaction has been suggested by Raunier et al. as a pathway to forming urea, based on their irradiation studies of solid isocyanic acid (Raunier et al. 2004). Multiconfigurational methods were used again to calculate the energy of the system whilst scanning over the CN distance between the radicals.

The potential energy curve for the singlet spin configuration is shown by the dark grey curve in Fig. 6. The well at 1.4 Å corresponds to the formation of urea via radical–radical recombination and has a depth of roughly 400 kJ mol^{-1}, which is in line with experimental data for the formation of a CN bond. The barrier at 2.4 Å is caused by the rearrangement of the formamide radical, which, at long interradical distances, had optimized to a structure, similar to isocyanic acid; see the inset in Fig. 6.

The behaviour of the singlet state beyond 4 Å deviated from what was expected due to significant convergence problems. Multiconfigurational methods, RASSCF in particular, are not blackbox methods. Unfortunately, a suitable active space to describe the long-range singlet state was not found. Therefore, it was decided to perform a triplet state scan as well. At infinite separation, the triplet and singlet states will be degenerate, deviating only at short range. The results of this scan are given by the lighter trace in Fig. 6. The triplet scan does not yield urea like the singlet state scan does, but behaves much better at long range. If the two curves are overlaid using the triplet results at long range and the singlet at short range, then they show that urea can be formed with a minimal barrier of only 4 kJ mol^{-1}, which occurs at 3.8 Å. The smaller barrier at 2.4 Å has a lower

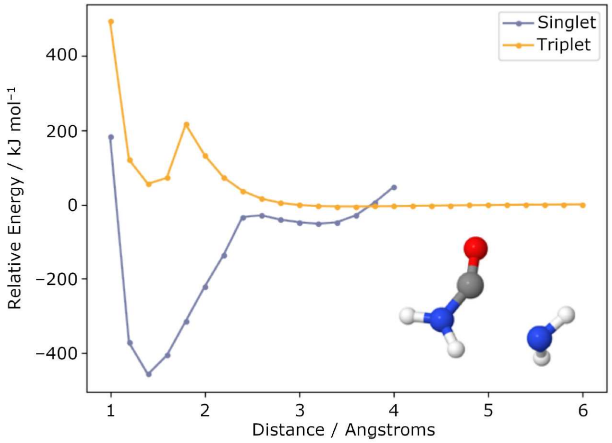

Figure 6. The potential energy curve for the addition of an amino radical to a formamide radical to give urea, as calculated by RASSCF in the singlet and triplet states with the energy of the triplet system at a 5-Å separation taken as the zero. Inset: The hydrogenated isocyanic acid-like structure seen in the system at long separations.

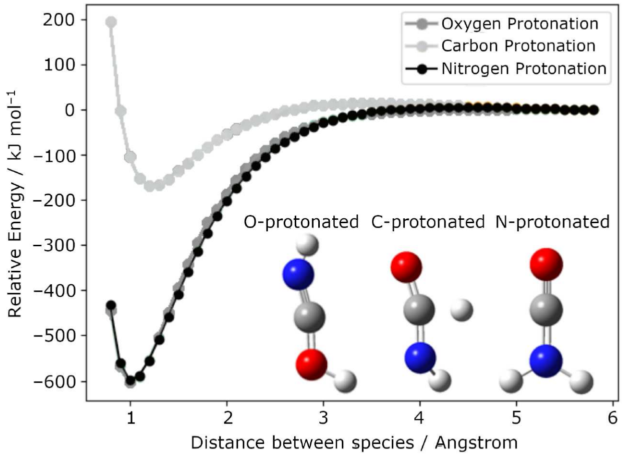

Figure 7. The potential energy curves for the addition of a proton to the oxygen, nitrogen, and carbon atoms in isocyanic acid with the lowest energy structures for, from the left- to right-hand side, the oxygen-protonated system, the carbon-protonated system, and the nitrogen-protonated system shown.

energy than the asymptotic energy and can therefore be classified as a submerged barrier. Therefore, this pathway presents the most facile means by which to produce urea in the ISM from neutral radical species generated from formamide and ammonia. However, this pathway, as those discussed above, only involves neutral molecules (either closed shell or radical) whereby it is noted that 100 per cent efficiency will depend on a spin flip. In light of this, further plausible routes were investigated.

3.3 Charged pathway

In Section 3.2, it was noted that the long range structure observed in the reaction between the formamide and amino radicals was that of neutral hydrogenated isocyanic acid. However, instead of hydrogenation, protonation could be occurring. Isocyanic acid (HNCO) has been detected in the ISM and can be formed from simple building blocks like atomic nitrogen and CO (Snyder & Buhl 1972; Buhl, Snyder & Edrich 1973; Nourry, Zins & Krim 2015). It has been used in the study of the formation of urea in irradiation studies, where its irradiation is shown to lead to the formation of formamide and urea (Ferus et al. 2018; Raunier et al. 2003, 2004). In addition, it has been shown to be a product of the dissociation of formamide and has even been suggested to be a catalyst for the formation of H_2 in the ISM (Lundell, Krajewska & Räsänen 1998; Duvernay et al. 2005; Haupa, Tarczay & Lee 2019). Moreover, there is a clear correlation with the abundances of formamide (Bisschop et al. 2007; López-Sepulcre et al. 2015). There is ample evidence of HNCO molecules functioning as an imine base, both in the gas phase and in the solid state (Dekock & Jasperse 1983; Hop et al. 1989; Hunter & Lias 1997; Hudson, Khanna & Moore 2005; Gupta et al. 2013; Bouchoux 2018; Marcelino et al. 2018). The proton affinity of HNCO is higher than that of water, so that one would expect protonation to occur even in water-based ices (Dekock & Jasperse 1983; Bouchoux 2018). Thus, in this section, calculations starting from protonated isocyanic acid are reported. Only DFT calculations were performed on these reactions, since multiconfigurational effects can be assumed to be small for these non-radical charged species. The first step that was investigated is the *protonation* of isocyanic acid. There are multiple options for protonation in this case: Protonation can occur on the nitrogen, carbon, or oxygen atoms. Hereby, we note that N-protonated isocyanic acid has been detected in laboratory experiments and in the ISM in the dense core L483 with a more tentative detection towards Sgr B2(N) (Hudson et al. 2005; Gupta et al. 2013; Marcelino et al. 2018). Moreover, O-protonated isocyanic acid has also been detected in laboratory experiments (Lattanzi et al. 2012). The potential energy curves for protonating on each of these atoms is shown in Fig. 7. Protonation on the nitrogen and oxygen atoms is barrierless. The well depths are 603.1 and 603.9 kJ mol^{-1}, respectively, making them equally likely. Protonation on the carbon atom, however, is not barrierless, but requires an energy input of 14.4 kJ mol^{-1}. It also results in a much less stable species, with a well depth of only 172.8 kJ mol^{-1}, making it the least likely of the three pathways. Nitrogen protonation is the product that most naturally leads on to the formation of urea as it creates one of the amino groups found in urea. None the less, the similarity in energies for the nitrogen- and oxygen-protonated species means that the oxygen-protonated species could also be formed. The latter is the species we will consider first.

The dark grey trace in Fig. 8 shows the reaction between ammonia and the oxygen protonated variant of protonated isocyanic acid. This reaction is barrierless and the protonated urea product is 85.1 kJ mol^{-1} lower in energy than the well-separated reactants (Fig. 8). It is also noted that the angle between the incoming ammonia and the isocyanic acid remains wider than the equilibrium angle. Obviously, the reaction of ammonia with an oxygen-protonated species will not lead to urea directly. Instead, the oxygen-protonated species will also have to undergo tautomerization (Fig. 9, upper panel) after the loss of a proton from ammonia, to yield the target product urea. If this tautomerization goes *via* a one-step process, as in panel (a) in Fig. 9, then there is a barrier of 130 kJ mol^{-1}. However, the tautomerization could also occur via a series of steps, as outlined in the lower panel (b) of Fig. 9. In this case, there is no barrier in the addition of a proton to the NH group. Moreover, this reaction is exothermic by almost 700 kJ mol^{-1}. The subsequent abstraction of a proton from OH^+ requires an energy input of 636.7 kJ mol^{-1}, consistent with this type of bond, making this process unlikely (Blanksby & Ellison 2003). However, as these process are expected to be occurring on an ice surface or in an ice, the effect of water ice on this step was considered as well. When water was present, in the form of three explicit water molecules to receive the removed proton, the

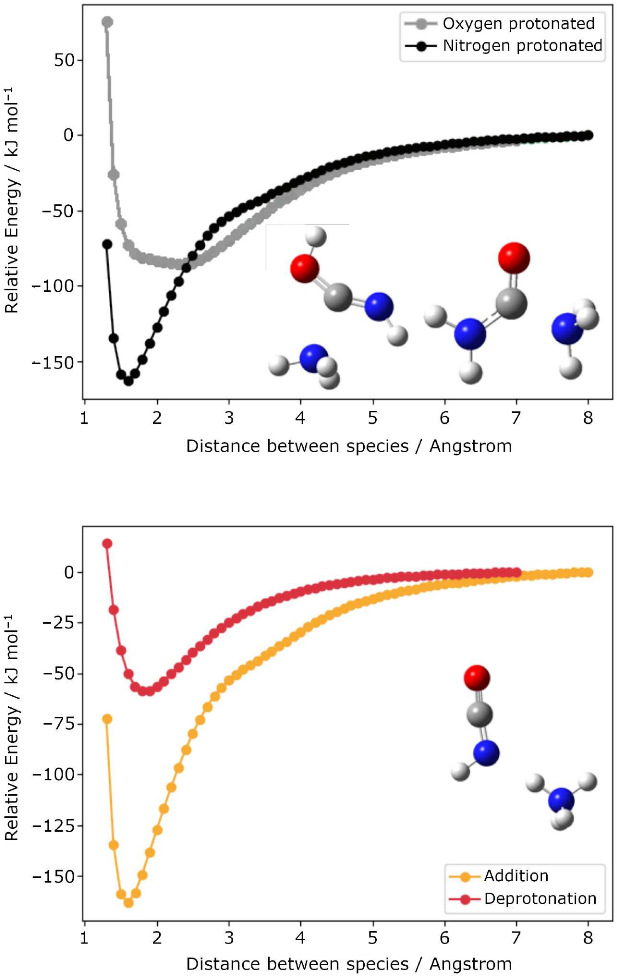

Figure 8. Upper panel: the potential energy curves for the addition of ammonia to the oxygen-protonated isocyanic acid and the nitrogen-protonated species with the lowest energy structures for each system shown. Lower panel: the potential energy curves for the addition of ammonia to the nitrogen-protonated species and the deprotonation of the nitrogen-protonated isocyanic acid by ammonia with the lowest energy structure for the deprotonation shown.

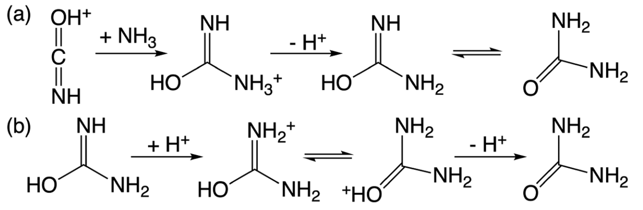

Figure 9. Upper panel: the reaction scheme for the addition of NH_3 to oxygen protonated isocyanic acid and the subsequent tautomerization of the product to give protonated urea (tautomerization 1). Lower panel: an alternative route for the tautomerization needed to form protonated urea from oxygen-protonated isocyanic acid (tautomerization 2).

energy input was reduced significantly to only 48 kJ mol^{-1} (0.5 eV), which could much more easily be supplied under ISM conditions (see Fig. 10). On the other hand, the overall step was still endothermic, albeit by 28 kJ mol^{-1}. However, as the barrier is comparatively small, some degree of conversion back to the protonated species could be anticipated, leading to a mixture of both species being present.

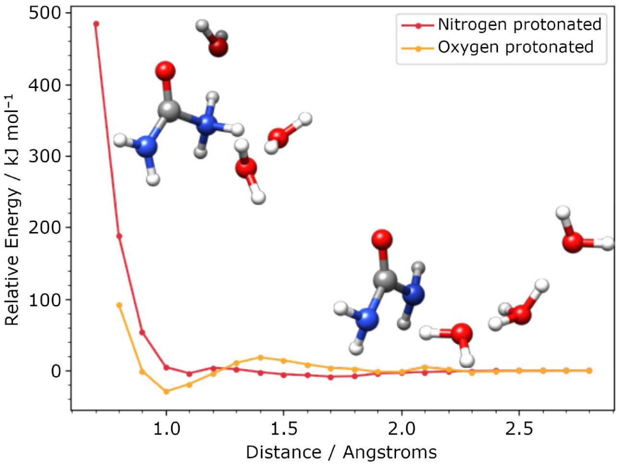

Figure 10. The potential energy curves the deprotonation of nitrogen and oxygen protonated urea, as calculated using DFT with water included in the system to mimic an ice mantle where the energy at an inter species distance of 5 Å is the zero. The insets show the structures of the nitrogen-protonated species before and after deprotonation.

Next, the addition of ammonia to the nitrogen-protonated species was considered. The upper panel of Fig. 8 shows that, if ammonia reacts with nitrogen-protonated isocyanic acid, the addition proceeds barrierlessly and has a well depth of 171.9 kJ mol^{-1}, 87 kJ mol^{-1} lower in energy than for addition to the oxygen-protonated species. The alternative reaction, where ammonia simply deprotonates the protonated isocyanic acid species, is also barrierless, but has a much shallower well of 57.4 kJ mol^{-1}, making the addition reaction the more energetically favourable of the two. Just as the oxygen-protonated species needs to undergo deprotonation to form urea, so does the nitrogen-protonated species. This process is barrierless and has a calculated dissociation energy of 636.7 kJ mol^{-1}. As with the oxygen-protonated species, this bond could be broken by Ly α radiation, but would require the protonated urea species to be in an area of a cloud, where such radiation is available. Alternatively, the deprotonation could occur *via* recombination with an electron from the gas phase. At present, all potential deprotonation methods have not been explored. As in the previously discussed oxygen-protonated case, there is also the possibility that ice species capable of hydrogen bonding will help mediate the deprotonation, and so reduce the energy input required. In order to test this, an analogous scan calculation was performed as for the oxygen-protonated species, with three explicit water molecules included to act as proton acceptors. As shown in Fig. 10, the presence of water vastly reduces the amount of energy required to deprotonate urea to only 7.8 kJ mol^{-1}. When the ice is included in the system, the lowest energy structure actually becomes neutral urea with the proton shared between the water ice molecules. This strongly suggests that the deprotonation would be essentially barrierless under these conditions.

4 CONCLUSIONS

Our calculations, carried out to probe the feasibility of the mechanism for the formation of urea proposed by Förstel et al. (2016), shown in Fig. 2 and equations (2) and (3), suggest that these are not an ISM-compatible routes:

$$\mathrm{NH_2CHO + NH_3 \longrightarrow (NH_2)_2CO + H_2}, \qquad (2)$$

$$NH_2CO\cdot + NH_3 \longrightarrow (NH_2)_2CO + H\cdot. \qquad (3)$$

The direct reaction of formamide and ammonia is endothermic, both when simulated in the gas phase and when simulated with water molecules as an ice mimic. Inspection of the optimized structures showed that the CH bond on formamide and one of the NH bonds in ammonia would not break to form urea and dihydrogen. Unfortunately, no transition state was identified, but it was be expected to be substantial. The nature of the ISM therefore makes this particular formation reaction unlikely. The single radical route (equation 3) presented initially a more feasible pathway. The formation of the formamide radical was found to be barrierless and the dissociation energy could be overcome by high-energy UV radiation. The subsequent reaction between the formamide radical and ammonia showed urea to be a stable product, but a reaction barrier of 282 kJ mol^{-1} was found in addition to the products being 20 kJ mol^{-1} higher in energy than the reactants. The barrier height combined with the endothermicity of the reaction makes this pathway unlikely under ISM conditions.

In light of these conclusions, an alternative single radical reaction (equation 4) was also tested using multiconfigurational methods:

$$NH_2CHO + NH_2\cdot \longrightarrow (NH_2)_2CO + H\cdot. \qquad (4)$$

However, this reaction was found to progress through a high-energy tetrahedral intermediate, resulting in a reaction barrier of 150 kJ mol^{-1}. While this barrier is lower than that for the previous single radical reaction, it is still too high for this to represent any kind of major formation route for urea in the ISM.

Instead, our conclusions are that the formation of urea in the ISM can either be described by either a radical–radical reaction or a reaction involving charged species. The most promising radical-containing reaction for the formation of urea from formamide and ammonia is the radical–radical reaction given in equation (5). This particular radical–radical reaction has previously been suggested and, at present, constitutes a major formation pathway for urea in astrochemical models (Garrod et al. 2008). This confirmation of its feasibility is therefore comforting:

$$NH_2CO. + NH_2\cdot \longrightarrow (NH_2)_2CO. \qquad (5)$$

This reaction can progress with a barrier of only 4 kJ mol^{-1}, one low enough that it is not prohibitive under ISM conditions, particularly when one considers the barriers to diffusion across the surface, which are likely to be greater than 4 kJ mol^{-1}, meaning that should the two species meet reacting is more achievable than further movement across the surface. One remaining issue with this particular route is that its efficiency does rely on the possibility of a spin flip from a triplet state at long range to a singlet shorter distances. To truly understand the importance of this pathway, further efforts ought to be directed to assessing this feasibility of this.

The most likely pathway using charged species, involves isocyanic acid protonated on the nitrogen atom. This is in agreement with available literature data, both for the gas phase as for the solid state (Dekock & Jasperse 1983; Hop et al. 1989; Hunter & Lias 1997; Hudson et al. 2005; Gupta et al. 2013; Bouchoux 2018; Marcelino et al. 2018). This species then reacts barrierlessly with ammonia to form protonated urea. Abstraction of the proton to form urea itself requires the presence of molecules, which are capable of hydrogen bonding. If water is used for these, then the NH deprotonation energy input becomes 7.8 kJ mol^{-1}. Moreover, the reaction becomes exothermic overall. Given the small nature of this barrier, then this route is at least as promising, if not more so, than the radical–radical pathway. Presently, it is not thought that a great deal of attention has been given to ion–molecule reactions on dust grain surfaces and so this result may suggest that further exploration could be worthwhile.

ACKNOWLEDGEMENTS

The authors would like to thank the Department of Chemistry at Sheffield for funding, and Rob Garrod for his comments and helpful discussion.

DATA AVAILABILITY

The data underlying this paper are available in the article and in its online supplementary material.

REFERENCES

Alberts B., Johnson A., Lewis J., Raff M., Roberts K., Walter P., 2002, Molecular Biology of the Cell, 4th edition, Garland Science, New York

Altwegg K. et al., 2016, Sci. Adv., 2, e1600285

Ashfold M. N. R., Ingle R. A., Karsili T. N. V., Zhang J., 2019, Phys. Chem. Chem. Phys., 21, 13880

Becke A. D., 1993, J. Chem. Phys., 98, 5648

Belloche A., Garrod R. T., Müller H. S. P., Menten K. M., Medvedev I., Thomas J., Kisiel Z., 2019, A&A, 628, A10

Bisschop S. E., Fuchs G. W., van Dishoeck E. F., Linnartz H., 2007, A&A, 474, 1061

Blanksby S. J., Ellison G. B., 2003, Acc. Chem. Res., 36, 255

Bouchoux G., 2018, Mass Spectrom. Rev., 37, 533

Buhl D., Snyder L. E., Edrich J. L., 1973, Nature, 243, 513

Butscher T., Duvernay F., Rimola A., Segado-Centellas M., Chiavassa T., 2017, Phys. Chem. Chem. Phys., 19, 2857

Butscher T., Duvernay F., Danger G., Torro R., Lucas G., Carissan Y., Hagebaum-Reignier D., Chiavassa T., 2019, MNRAS, 486, 1953

Dekock R. L., Jasperse C. P., 1983, Inorg. Chem., 22, 3839

Dulieu F., Nguyen T., Congiu E., Baouche S., Taquet V., 2019, MNRAS, 484, L119

Duvernay F., Trivella A., Borget F., Coussan S., Aycard J. P., Chiavassa T., 2005, J. Phys. Chem. A, 109, 11155

Ehrenfreund P., Charnley S. B., 2000, ARA&A, 38, 427

Ferus M. et al., 2018, A&A, 616, 1

Förstel M., Maksyutenko P., Jones B. M., Sun B.-J., Chang A. H. H., Kaiser R. I., 2016, Chem. Commun., 52, 741

Fourikis N., Takagi K., Morimoto M., 1974, ApJ, 191, L139

Fray N. et al., 2016, Nature, 538, 72

Frisch M. J., Head-Gordon M., Pople J. A., 1990a, Chem. Phys. Lett., 166, 275

Frisch M. J., Head-Gordon M., Pople J. A., 1990b, Chem. Phys. Lett., 166, 281

Frisch M. J., et al., 2009, Gaussian 09 Revision D.01, Gaussian Inc, Wallingford CT

Garrod R. T., Herbst E., 2006, A&A, 457, 927

Garrod R. T., Weaver S. L. W., 2013, Chem. Rev., 113, 8939

Garrod R. T., Weaver S. L. W., Herbst E., 2008, ApJ, 682, 283

Gorai P., Das A., Majumdar L., Chakrabarti S. K., Sivaraman B., Herbst E., 2017, Mol. Astrophys., 6, 36

Gupta H., Gottlieb C. A., Lattanzi V., Pearson J. C., McCarthy M. C., 2013, ApJ, 778, L1

Haupa K. A., Tarczay G., Lee Y. P., 2019, J. Am. Chem. Soc., 141, 11614

Hayatsu R., Studier M. H., Moore L. P., Anders E., 1975, Geochim. Cosmochim. Acta, 39, 471

Holdship J. et al., 2019, ApJ, 878, 64

Hollis J. M., Lovas F. J., Remijan A. J., Jewell P. R., Ilyushin V. V., Kleiner I., 2006, ApJ, 643, L25

Hop C. E. C. A., Holmes J. L., Ruttink P. J. A., Schaftenaar G., Terlouw J. K., 1989, Chem. Phys. Lett., 156, 251

Hudson R. L., Khanna R. K., Moore M. H., 2005, ApJS, 159, 277
Hunter E. P. L., Lias S. G., 1997, J. Phys. Chem. Ref. Data, 27, 413
Jeilani Y. A., Fearce C., Nguyen M. T., 2015, Phys. Chem. Chem. Phys., 17, 24294
Jørgensen J. K., Favre C., Bisschop S. E., Bourke T. L., van Dishoeck E. F., Schmalzl M., 2012, ApJ, 757, L4
Kaňuchová Z., Urso R. G., Baratta G. A., Brucato J. R., Palumbo M. E., Strazzulla G., 2016, A&A, 585, A155
Kinne-Saffran E., Kinne R. K., 1999, Am. J. Nephrology, 19, 290
Knowles P. J., Werner H.-J., 1985, Chem. Phys. Lett., 115, 259
Krishnan R., Binkley J. S., Seeger R., Pople J. A., 1980, J. Chem. Phys., 72, 650
Lattanzi V., Thorwirth S., Gottlieb C. A., Mccarthy M. C., 2012, J. Phys. Chem. Lett., 3, 3420
Lee C., Yang W., Parr R. G., 1988, Phys. Rev. B, 37, 785
López-Sepulcre A. et al., 2015, MNRAS, 449, 2438
Lundell J., Krajewska M., Räsänen M., 1998, J. Phys. Chem. A, 102, 6643
McLean A. D., Chandler G. S., 1980, J. Chem. Phys., 72, 5639
Marcelino N., Agúndez M., Cernicharo J., Roueff E., Tafalla M., 2018, A&A, 612, 1
Miller S. L., Orgel L. E., 1974, The Origins of Life on the Earth. Prentice-Hall, New Jersey
Miller S. L., Urey H. C., 1959, Science, 130, 245
Nourry S., Zins E. L., Krim L., 2015, Phys. Chem. Chem. Phys., 17, 2804
Öberg K. I., 2016, Chem. Rev., 116, 9631
Orgel L. E., 1986, J. Theor. Biol., 123, 127
Pettersson M., Khriachtchev L., Jolkkonen S., Räsänen M., 1999, J. Phys. Chem. A, 103, 9154
Raunier S., Chiavassa T., Marinelli F., Allouche A., Aycard J. P., 2003, Chem. Phys. Lett., 368, 594
Raunier S., Chiavassa T., Duvernay F., Borget F., Aycard J. P., Dartois E., D'Hendecourt L., 2004, A&A, 416, 165
Redondo P., Barrientos C., Largo A., 2013, ApJ, 780, 181
Remijan A. J. et al., 2014, ApJ, 783, 77
Robertson M. P., Miller S. L., 1995, Nature, 375, 772
Rubin R. H., Swenson G. W. J., Benson R. C., Tigelaar H. L., Flygare W. H., 1971, ApJ, 169, L39
Sharma M. K., 2019, Mol. Astrophys., 15, 1
Shaw A. M., 2007, Astrochemistry: From Astronomy to Astrobiology, John Wiley & Sons, Chichester UK
Snyder L. E., Buhl D., 1972, ApJ, 177, 619
Song L., Kästner J., 2016, Phys. Chem. Chem. Phys., 18, 29278
Spezia R., Jeanvoine Y., Hase W. L., Song K., Largo A., 2016, ApJ, 826, 107
Tielens A. G. G. M., 2013, Rev. Mod. Phys., 85, 1021
Wakelam V., Loison J.-C., Hickson K. M., Ruaud M., 2015, MNRAS, 453, 48
Werner H., Knowles P. J., 1985, J. Chem. Phys., 82, 5053
Werner H.-J., Knowles P. J., Knizia G., Manby F. R., Schütz M., 2012, Wiley Interdiscip. Rev.: Comput. Mol. Sci., 2, 242
Wöhler F., 1828, Ann. Phys. Chem., 88, 253
Yanai T., Tew D. P., Handy N. C., 2004, Chem. Phys. Lett., 393, 51
Zhao L. et al., 2019, Chem. Phys. Chem., 20, 1437

SUPPORTING INFORMATION

Supplementary data are available at *MNRAS* online.

SI.pdf

Please note: Oxford University Press is not responsible for the content or functionality of any supporting materials supplied by the authors. Any queries (other than missing material) should be directed to the corresponding author for the article.

This paper has been typeset from a TEX/LATEX file prepared by the author.